Characterizing formation of interfacial domain wall and exchange coupling strength in laminated exchange coupled composites

H.-C. Hou[1], B. J. Kirby[2], K. Z. Gao[3], and C.-H. Lai*[1]

[1] *Department of Materials Science and Engineering, National Tsing Hua University, Hsinchu, 30013, Taiwan*

[2] *NIST Center for Neutron Research,National Institute of Standards and Technology, Gaithersburg, 20899*

[3] *Seagate Technology, Bloomington, Minnesota 55435*

We have studied the *N*-dependent switching behavior of composite magnets, comprised of a hard CoPtCr-SiO_2 (CPCS) film and a laminated soft $[Pt/CPCS]_N$ multilayer. First order reversal curve (FORC) magnetometry provides evidence of interfacial domain wall (iDW) assisted reversal for $N \geq 5$. The magnetic depth profiles determined from polarized neutron reflectometry (PNR) explicitly demonstrate that the composite magnets are more rigidly coupled for N=3 than for N=7, and suggest that for N=7 reversal occurs via formation of iDW. By fitting the PNR profile into the energy surface calculations, we can further deduce the vertical coupling strength in the laminated soft layer.

*corresponding author: Chih-Huang Lai, chlai@mx.nthu.edu.tw

Two-phase composite magnets have drawn a great deal of attention due to the potential for ultrahigh areal density recording media.[1,2,3] In particular, exchange coupled composite (ECC) media, composed of exchange coupled soft and hard layers with well-isolated granular structures are being pursued to optimize the balance between writeability and thermal stability, and to achieve superior recording performance.[4,5] The reversal behavior of such composite magnetic films can be described by a phase diagram with parameters including layer thicknesses, anisotropy constants, and interfacial coupling strengths.[6,7] It has been reported that when the thickness of the soft phase is increased such that is larger than the associated exchange length, spins distant from the hard/soft interface decouple from the hard layer, and the switching process of the composite film changes from a coherent reversal to an incoherent exchange spring reversal.[8] The latter case is characterized by decoupled spins in the soft layer responding to an opposing applied field by rotating and nucleating an interfacial domain wall (iDW) that penetrates toward the hard layer, assisting overall magnetization reversal.

Although the iDW assisting reversal of magnetic heterostructures have been widely studied theoretically and with micromagnetic simulations;[9,10] it is still a challenge to reveal the formation of interfacial domain walls and the layer-to-layer coupling in perpendicular composite films primarily due to the difficulties of differentiating the coupled soft and hard phases by standard magnetometry techniques. On the other hand, the first order reversal curve (FORC)[11] analysis that can probe the interaction and switching field of coupled magnetic layers may provide an opportunity to identify the iDW assisting reversal in composite magnets. In addition, characterization of the exchange coupling inside the layers of a composite magnet is essential to further understand its reversal. The polarized neutron reflectometry (PNR)[12] has been used to probe magnetic depth profiles, which can provide the information for the exchange coupling, in heterogeneous structures such as exchange bias systems,[13,14,] exchange springs,[15,16,17]and graded anisotropy multilayers.[18]

In this Letter, we utilize experimental results of FORC and PNR measurements and fit data into energy surface model calculations[19,20,21] to shed light on the magnetization reversal behavior and the extent of the interfacial coupling field in exchange coupled composites. The proposed approach can enable researchers to characterize advanced multilayered media.

Multilayers with structure of Si substrate / 200 nm SiO_2 / 3 nm Ta / 7 nm Pt / 15 nm Ru / 12 nm CoPtCr-SiO_2 (CPCS) / [0.7 nm Pt / 1.1 nm CPCS]$_{N=0,3,5,7}$ / 2 nm Pt were prepared by DC sputtering. All CPCS layers were deposited by reactive sputtering with a working gas mixture of Ar and 0.5% O_2. Consequently, the samples exhibit columnar growth and clear oxide segregation at the grain boundaries, as revealed by the transmission electron microscopy (TEM) images of the sample with N=5 shown in Fig. 1(a). The 12 nm CPCS layer constitutes the hard layer of the ECC, while the Pt/CPCS multilayer is the soft layer.[22] Samples were prepared with different repetition number *N* (0,3,5,7) of the soft bilayer and are denoted as PMR (*N*=0, pure hard sample), ECC-N3, ECC-N5, and ECC-N7, respectively.

To investigate the reversal behaviors, the major hysteresis loops and FORCs were measured by using a vibrating sample magnetometer (VSM); the FORCs were measured at room temperature, while the major loops were measured at 5 K to prevent thermal fluctuation. For the FORC measurements, samples were saturated positively to a particular reversal field H_R, and then the magnetization was measured under increasing applied field H back to saturation, thereby tracing out a single FORC.[11,23] This process was repeated for successively smaller values of H_R creating a family of FORCs. A FORC distribution was defined as a mixed second-order derivative:

$$F \equiv -\partial^2 (H, H_R)/2\ \partial H \partial H_R$$

For the granular system, we apply a simple coordinate transformation to plot F in coordinates of H_C and H_B, where $H_C = (H - H_R)/2$ describes the intrinsic coercivity of the system, and $H_B = (H + H_R)/2$ describes the local interaction fields, respectively.[23,24]

Room temperature PNR measurements were conducted using the NG-1 Reflectometer at the NIST Center for Neutron Research, and Asterix at the Los Alamos Neutron Science Center. The incident neutron beam was polarized to be alternately spin-up (+) or spin-down (-) with respect to an in-plane applied field, and an analyzer was used to determine the spin state of the scattered beam.[25] No significant spin-flip or off-specular scattering was detected (or expected), thus we discuss only measurements of non spin-flip specular reflectivities as functions of scattering vector along the surface normal (z) direction, $R^{++}(Q_z)$ and $R^{--}(Q_z)$. These spin-dependent reflectivities are functions of the spin-dependent real space scattering length density profile:

$$\rho^{\pm\pm}(z) = \rho_N(z) \pm C{*}M(z)$$

where ρ_N is indicative of the nuclear composition, M is the in-plane projection of the sample magnetization parallel to the applied field, and C is a constant.[26] Therefore, the sample magnetization is manifest as a divergence of R^{++} and R^{--}. Depth profiles were determined by model fitting of R^{++} and R^{--} with exact dynamical calculations,[12] using the Refl1D software package.[27]

Fig. 1(b) shows the coercivity (H_c), remanent coercivity (H_{cr}), and saturation field (H_s) as functions of soft layer repetition number, N, as determined from low-temperature easy-axis major hysteresis loop measurements. H_c, H_{cr} and H_s decrease with increasing N, leveling off to constant values for $N \geq 5$. Micromagnetic simulations have shown that once the thickness of the soft layer exceeds the intrinsic exchange length of the material, further thickening the soft layer does not appreciably reduce H_s and H_{cr}.[8] Therefore, the results shown in Fig. 1(b) suggest that for $N \geq 5$, the samples exhibit exchange-spring magnetization reversal characterized by formation of a full iDW in the soft layer. The significant discrepancy between H_c and H_{cr} for $N \geq 5$ implies reversible magnetization, also consistent with exchange spring formation.[28,29] In contrast, the values of H_c and H_{cr} are essentially the same for $N \leq 3$, suggesting that spins reverse coherently in those samples, and do not contribute a reversible portion to the demagnetization curve.

The FORC distributions of the samples with different N repetitions of the soft layer are shown in Fig. 2. Each sample exhibits a "wishbone" with two branches along H_C and H_B. This feature is characteristic of well-separated magnetic elements (grains in this case), as has been reported for Ni nanopillar arrays.[23] Within the wishbone, the peak at the positive H_B intercept of the two branches can be attributed to a dominant dipolar field that motivates anti-parallel magnetization alignment between contiguous grains.[30] This peak, coupled with the evidence of grain boundaries with well-segregated SiO_2 shown in Fig. 1(a), indicates that inter-grain exchange coupling can be neglected, and that lateral domain wall motions play negligible roles in the switching behavior of these samples. This is an important point, as such domain wall motion could potentially mask evidence of vertical iDW formation.

The FORC distribution for the PMR sample, shown in Fig.2 (a), features a vertical band at $H_C = 0.5$ T and a strong peak at $H_B = 0.18$ T, corresponding to the intrinsic switching field and the positive bias field (i.e. dipolar coupling) of the system, respectively. Similar features can be seen in the FORC distribution for ECC-N3 (Fig. 2(b)), indicating that the $N = 3$ soft layer is rigidly coupled to the hard layer, and switches (like the PMR film) via coherent Stoner-Wohlfarth rotation. However, important differences emerge with increasing N. The FORC distributions for ECC-N5 and ECC-N7, are shown in Fig. 2(c) and 2(d) respectively, and both feature an extra $-H_B$ peak within the vertical band. This extra peak can be attributed to the existence of an iDW that expands from the top of the soft layer and becomes pinned by the hard layer at the hard / soft interface, results in the negative bias field. Therefore, the emergence of a second peak is indicative of an incomplete coupling of the hard and soft layers, implying that iDW assisted reversal occurs for $N \geq 5$.

To confirm our interpretation of the FORC features, specular PNR measurements were used to experimentally probe the depth-dependence of the magnetization characteristic for the $N = 7$ and $N = 3$ samples. Since the technique is insensitive to the component of the sample magnetization normal to the sample surface, scans were conducted as a function of increasing *in-plane* field after first saturating along the perpendicular easy axis direction. In this way we were able to probe the in-plane projection of the magnetization as it was pulled away from the easy axis. Figure 3 shows example fitted PNR spectra taken at low and high field for ECC-N7 (a-b) and ECC-N3 (e-f). The fitted data are plotted as spin asymmetry (the difference in R^{++} and R^{--} divided by the sum), a useful quantity for visualizing the magnetic contribution to the scattering. Pronounced field-dependent oscillations are observed, indicating sensitivity to evolution of the magnetic profile. The bottom of Fig. 3 shows the profiles determined from model fitting of the PNR data. The nuclear profiles (Figs. 3c and 3g) provide a structural reference for the magnetic profiles, with clear features corresponding to the hard CPCS layer, and the soft $[\mathrm{CPCS} / \mathrm{Pt}]_N$ multilayer. The intermixing may occur at the Pt / CPCS interfaces, and the measured Q_z range is insufficient to explicitly resolve the thin (0.7 nm) Pt spacer layers. Thus for both samples, the soft multilayer is modeled as a single "alloy" layer with higher ρ_N corresponding to the increased Pt concentration. For the model fitting, the nuclear (structural) parameters were held constant as a function of field while the magnetic parameters were allowed to vary. The hard / soft nuclear and magnetic interfaces are modeled as smooth Gaussian functions, and are not in general constrained to have the same width. The field-dependent magnetization profiles are shown in Figs. 3(d) and 3(h). As an increasing in-plane field is applied to ECC-N7, the magnetization of the $[\mathrm{CPCS} / \mathrm{Pt}]_7$ multilayer is initially larger than that of the pure CPCS layer, but as saturation is approached, the pure CPCS layer magnetization surpasses that of the multilayer, owing to the increased Pt content. Thus, the multilayer approaches saturation "faster" than does the CPCS layer, demonstrating that the multilayer is indeed significantly softer. Additionally, as field is increased, the *width* of the magnetic interface is initially a factor of ten larger than that of the nuclear interface, before the magnetic value converges to the nuclear value at 0.82 T - consistent with formation and annihilation of an exchange spring iDW. For ECC-N3, the field-dependent magnetization of the hard CPSC layer (Fig. 3h) is very similar to that of ECC-N7, but the soft multilayer of ECC-N3 is much harder than that of ECC-N7.

Since the two samples differ only in number of soft bilayer repeats (N), and do not otherwise differ in composition, the two samples should have identical magnetocrystalline anisotropy. Therefore, any differences in switching behavior are most likely attributable to exchange coupling. To determine the intrinsic exchange energies A of the pure CPCS and the $[\mathrm{CPCS} / \mathrm{Pt}]_N$ multilayer, we have performed energy surface modeling, an energy minimization technique used to determine the equilibrium magnetic configuration of particles in external applied field.[19,20,21] Figure 4 shows a comparison of the measured 0.05 T ECC-N7 profile to an energy surface calculation of the magnetic profile corresponding to $A = 6.5$ pJ m^{-1} for the hard CPCS layer, and $A = 2.2$ pJ m^{-1} for the soft $[\mathrm{CPCS} / \mathrm{Pt}]_7$ multilayer. The calculation produces a good match to the measured profile, indicating that insertion of the Pt laminate layers leads to a factor of four reduction in exchange energy.

Therefore, the observed decrease in multilayer hardness with increasing N can be understood in terms of interfacial exchange coupling between a layer with high intrinsic A (the CPCS), and an adjacent layer with significantly lower intrinsic A (the$[\mathrm{CPCS} / \mathrm{Pt}]_N$). When the low A layer is thinner than an exchange length L_E that defines the range of influence of the high A layer, the entirety of the low A layer rigidly couples to the high A layer, as in the case of ECC-N3. When the low A layer is thicker than L_E, an iDW can propagate from the loosely coupled low A spins distant from the high A / low A interface, leading to exchange spring reversal, as in the case of ECC-N7. From the flattening of H_c, H_{cr}, and H_s in Fig. 1b, we can infer that the transition between rigid magnet and exchange spring magnet occurs for $3 < N < 5$, implying that L_E is between 5-9 nm.

In summary, we have produced ECC multilayers with well-isolated grains comprised of a hard layer and a soft laminated multilayer, and have demonstrated that the collective magnetic behavior can be tuned from that of a rigid magnet to that of an exchange spring, which is experimentally revealed by using measurements of first order reversal curve magnetometry and polarized neutron reflectometry. By fitting the PNR profile into the energy surface calculations, we can further deduce the exchange energy in both of the hard layer and the laminated soft layer. Our proposed approaches can be used to characterize advanced multilayered media.

This research was supported by National Science Council of Republic of China under Grant No. NSC-101-2221-E-007-049 and the Hsinchu Science Park of Republic of China under Grant No. 101A16. We acknowledge use of the facilities at the Lujan Neutron Scattering Center at Los Alamos National Laboratory.

Figure captions

Fig.1 (color on-line) (a) TEM cross-sectional image of ECC film with $N = 5$; inset is the corresponding plan-view image (b) the summarization of the H_c, H_{cr} and H_s of PMR (N=0) and ECC film with various N measured at low temperature of 5 K.

Fig.2 (color on-line) FORCs contour plot of (a) PMR, (b) ECC-N3, (c) ECC-N5, and (d) ECC-N7; the dashed circle in (c) and (d) reveals the second peak at negative H_B, which is ascribed to the iDW motion.

Fig. 3 (color on-line) Fitted PNR data plotted as spin asymmetry and corresponding nuclear and field-dependent magnetic profiles for ECC-N7 (a-d) and ECC-N3 (e-h). Error bars correspond to ± 1 sigma.

Fig. 4 (color on-line) Depth profiles of magnetization polar angle of ECC-N7 with 0.05 T in-plane field calculated by energy surface model (Both hard and soft layers are divided into seven segments (1.8nm)); the experimental result obtained from PNR is also plotted in red dash line. The magnetization polar angle is deduced from the magnetic profile of 0.05 T normalized by the saturated profile (1.5 T).

Reference

[1] R. H. Victora and X. Shen, IEEE Trans. Magn. **41**, 2828 (2005).

[2] D. Suess T. Schrefl, R. Dittrich, M. Kirschner, F. Dorfbauer, G. Hrkac, and J. Fidler, J. Magn. Magn. Mater. **290–291**, 551 (2005).

[3] S. Li, K. Z. Gao, L. Wang, W. Zhu and X. Wang, U.S. Patent No. 7,846,564 (2005).

[4] J.-P. Wang, W. Shen, and S.-Y. Hong, IEEE Trans. Mag. **43**, 682 (2007).

[5] D. Suess , J. Lee, J. Fidler, and T. Schrefl, J. Magn. Magn. Mater. **321**, 545 (2009).

[6] G. Asti, M. Ghidini, R. Pellicelli, C. Pernechele, M. Solzi, F. Albertini, F.Casoli, S. Fabbrici, and L. Pareti, Phys. Rev. B, **73**, 094406 (2006).

[7] H.-C. Hou, M.-S. Lin, J.-W. Liao, T.-L. Wu, C.-H. Lai, R.-Z. Chen, J.-L. Lee, H.-J. Lin, F.-H. Chang, and J.-S. Yang, J. Appl. Phys. **105**, 07B729.(2009).

[8] A. Y. Dobin and H. J. Richter, Appl. Phys. Lett. **89**, 062512 (2006).

[9] E. Kneller and R. Hawig, IEEE Trans. Magn. **27**, 3588(1991).

[10] H. Kronmueller and D. Goll, Physica B **403**, 283 (2008).

[11] J. E. Davies, O. Hellwig, E. E. Fullerton, G. Denbeaux, J. B. Kortright, and K. Liu, Phys. Rev. B, **70**, 224434, (2004)

[12] C. F. Majkrzak et al., in Neutron Scattering From Magnetic Materials, edited by T. Chatterji (Elsevier Science, New York, 2005).

[13] M. R. Fitzsimmons, P. Yashar, C. Leighton, Ivan K. Schuller, J. Nogues, C. F. Majkrzak, and J. A. Dura, Phys. Rev. Lett. **84**, 3986 (2000).

[14] T. Hauet, J. A. Borchers, P. Mangin, Y. Henry, and S. Mangin, Phys. Rev. Lett., **96**, 067207 (2006).

[15] K. V. O'Donovan, J. A. Borchers, C. F. Majkrzak, O. Hellwig, and E. E. Fullerton, Phys. Rev. Lett. **88**, 067201 (2002).

---

[16] Y. Liu, S. G. E. te Velthuis, J.-S. Jiang, Y. Choi, S. D. Bader, A. A. Parizzi, H. Ambaye, and V. Lauter, Phys. Rev. B, **83**, 174418, (2011).

[17] M. R. Fitzsimmons, S. Park, K. Dumesnil, C. Dufour, R. Pynn, J. A. Borchers, J. J. Rhyne, and Ph. Mangin, Phys. Rev. B, **73**, 134413 (2006).

[18] B. J. Kirby, J. E. Davies, K. Liu, S.M.Watson, G. T. Zimanyi, R. D.Shull, P. A. Kienzle, and J. A. Borchers, Phys. Rev. B, **81**, 100405(2010).

[19] Kai-Zhong Gao, Eric D. Boerner, and H. Neal Bertram, Appl. Phys. Lett. **81**, 4008 (2002).

[20] Kai-Zhong Gao, Eric D. Boerner, and H. Neal Bertram, J. Appl. Phys. **93**, 6549 (2003).

[21] Kai-Zhong Gao and Mourad Benakli, Appl. Phys. Lett. **94**, 102506 (2009).

[22] H.-C. Hou, D. Suess, J.-W. Liao, M.-S. Lin, H.-J. Lin, F.-H. Chang, and C.-H. Lai, Appl. Phys. Lett., **98**, 262507 (2011).

[23] C. R. Pike, C. A. Ross, R. T. Scalettar, and G. Zimanyi, Phys. Rev. B, **70**, 134407 (2005).

[24] H.-C. Hou, J.-W. Liao, L.-W. Wang, R.-Z. Chen, C.-H. Chiu , H.-J. Lin, F.-H, Chang, and C.-H. Lai, Phys. J. Appl. Phys. **111**, 07B725 (2012).

[25] No analyzer was used for the 1.5 T PNR measurements, as we assumed the sample magnetization was essentially saturated along the applied field direction.

[26] $C = 2.853 \times 10^{-7}$, for M in kA m^{-1}, and ρ in nm^{-2}.

[27] B. J. Kirby, P. A. Kienzle, B. B. Maranville, N. F. Berk, J. Krycka, F. Heinrich, and C. F.Majkrzak, *Curr. Opin. Colloid Interface Sci.* **17**, 44 (2012).

[28] H. Fukunaga, J. Kuma, and Y. Kanai, IEEE Trans. Magn. **35**, 3235(1999).

[29] E. Girt, A. Yu. Dobin, B. Valcu, H. J. Richter, X.Wu, and T. P. Nolan, IEEE Trans.

Magn. **43**, 2166(2007).

[30] B. F. Valcu , D. A. Gilbert, and K. Liu, IEEE Trans. Magn. **47**, 2988(2011).

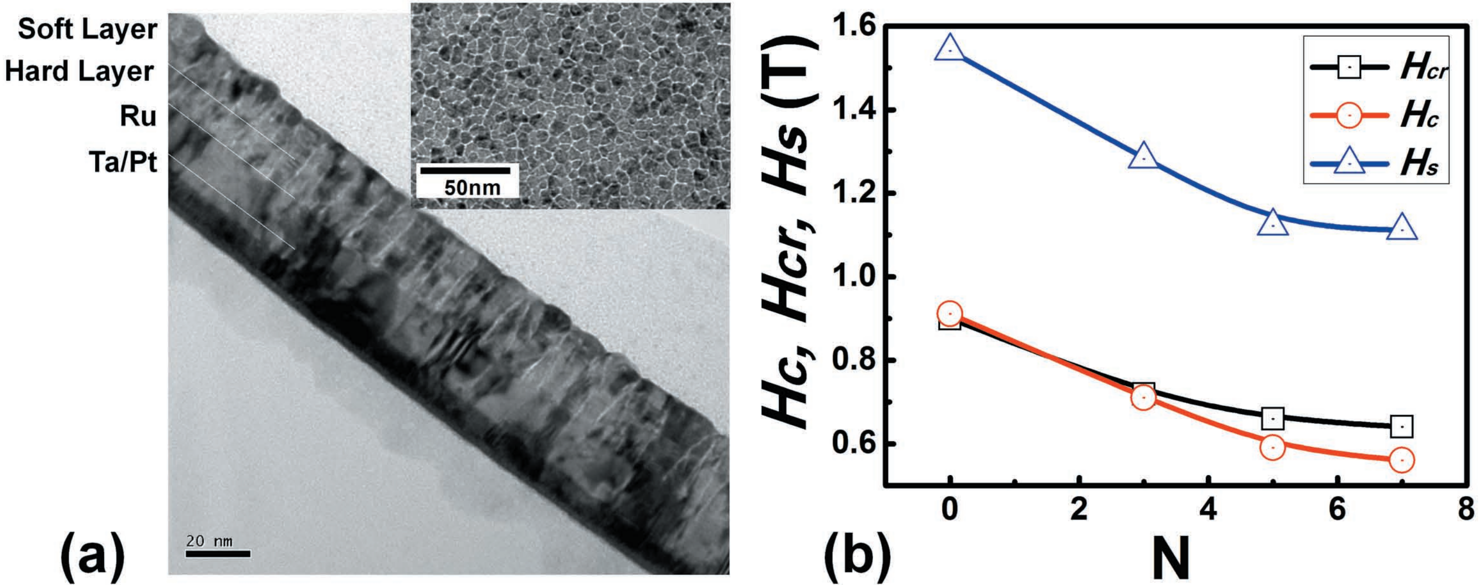

Soft Layer
Hard Layer
Ru
Ta/Pt
50nm
20 nm
(a)
1.6
1.4
1.2
1.0
0.8
0.6
0
2
4
6
8
N
Hc, Hcr, Hs (T)
Hcr
Hc
Hs
(b)

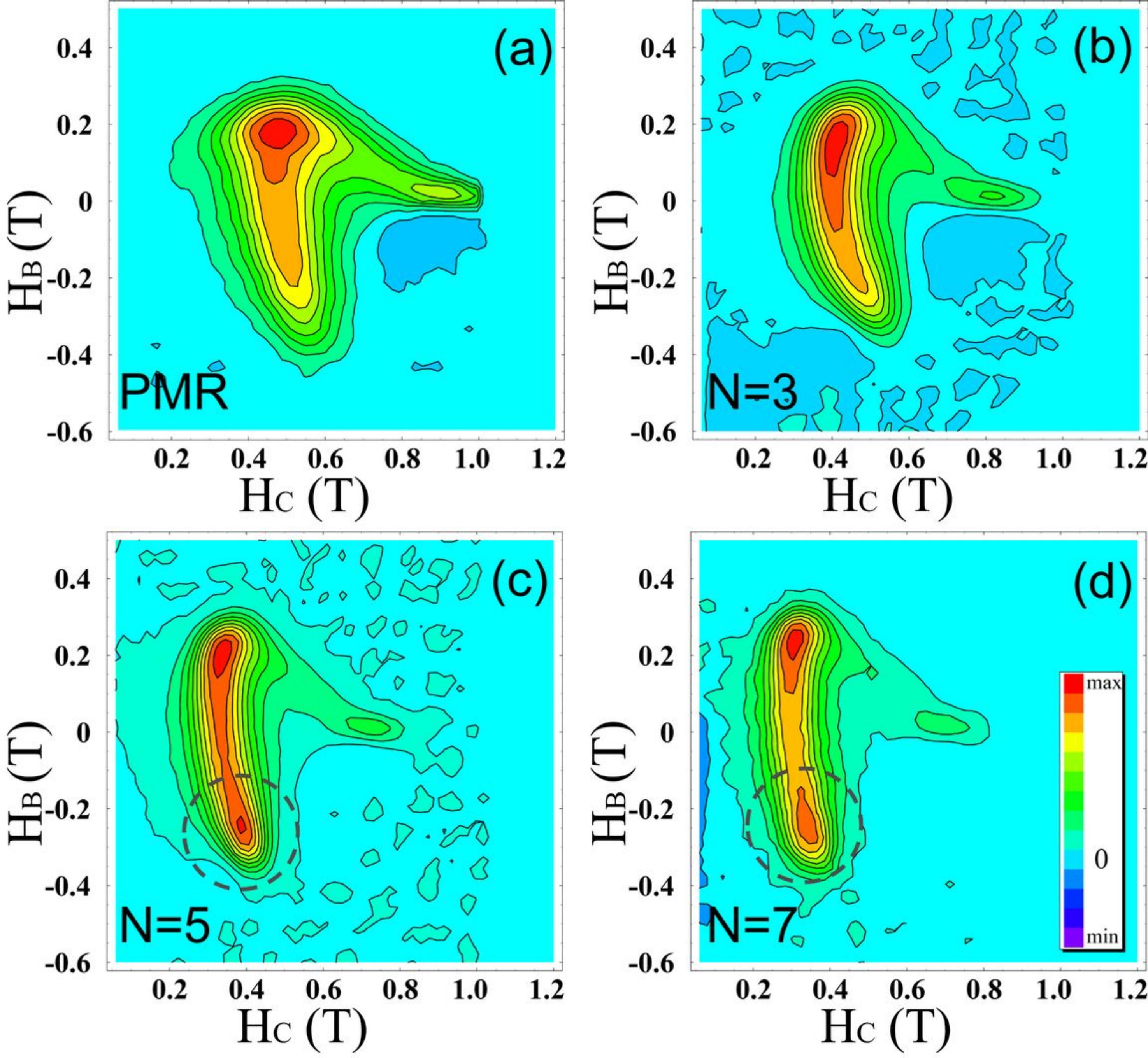

(a)
PMR
(b)
N=3
(c)
N=5
(d)
N=7
max
0
min
HB (T)
HC (T)
0.4
0.2
0
-0.2
-0.4
-0.6
0.2
0.4
0.6
0.8
1.0
1.2

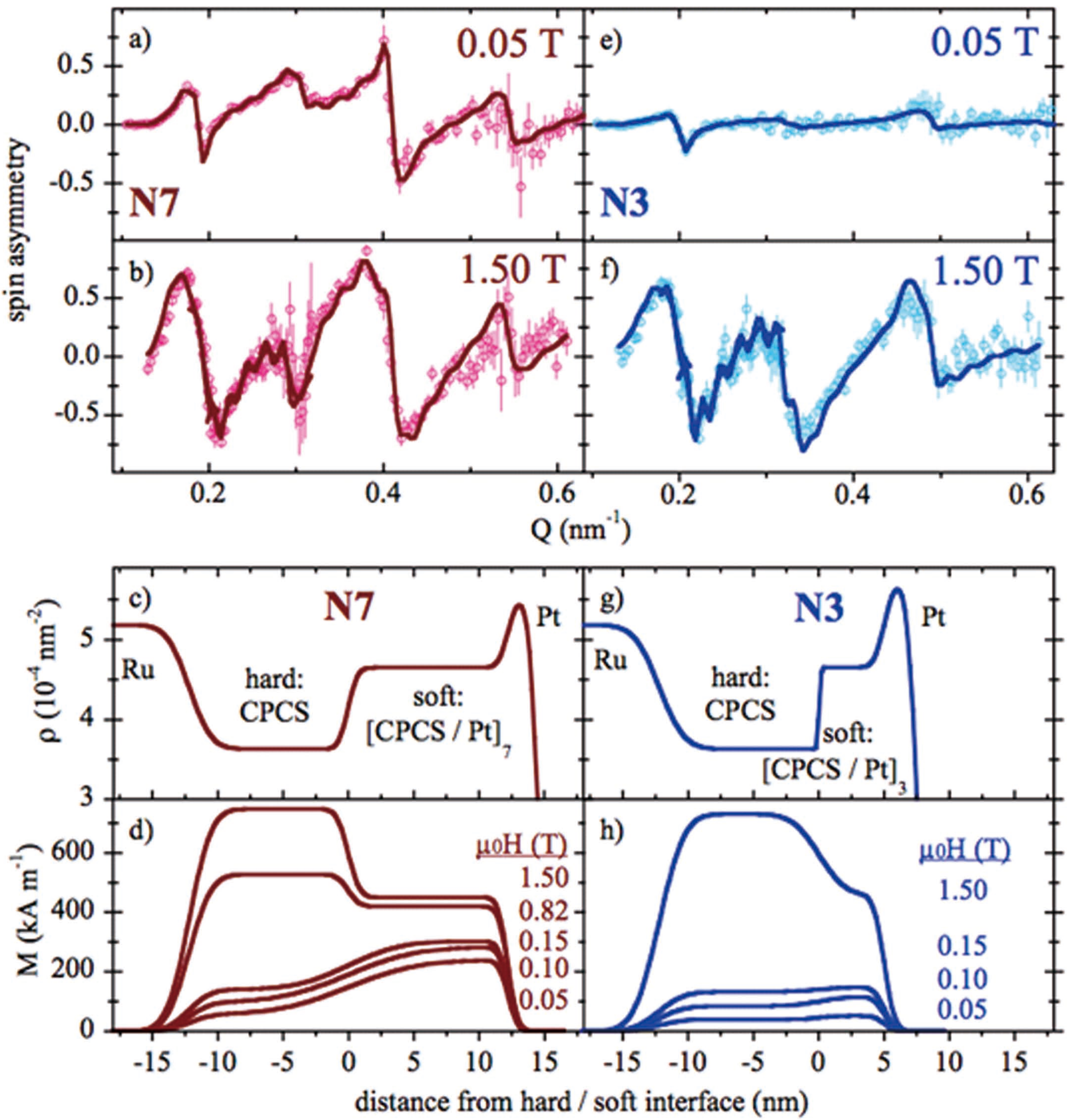

a)
0.05 T
N7
b)
1.50 T
e)
0.05 T
N3
f)
1.50 T
spin asymmetry
Q (nm^{-1})
c)
N7
Ru
hard:
CPCS
soft:
[CPCS / Pt]$_7$
Pt
g)
N3
Ru
hard:
CPCS
soft:
[CPCS / Pt]$_3$
Pt
ρ (10^{-4} nm^{-2})
d)
μ0H (T)
1.50
0.82
0.15
0.10
0.05
h)
μ0H (T)
1.50
0.15
0.10
0.05
M (kA m^{-1})
distance from hard / soft interface (nm)

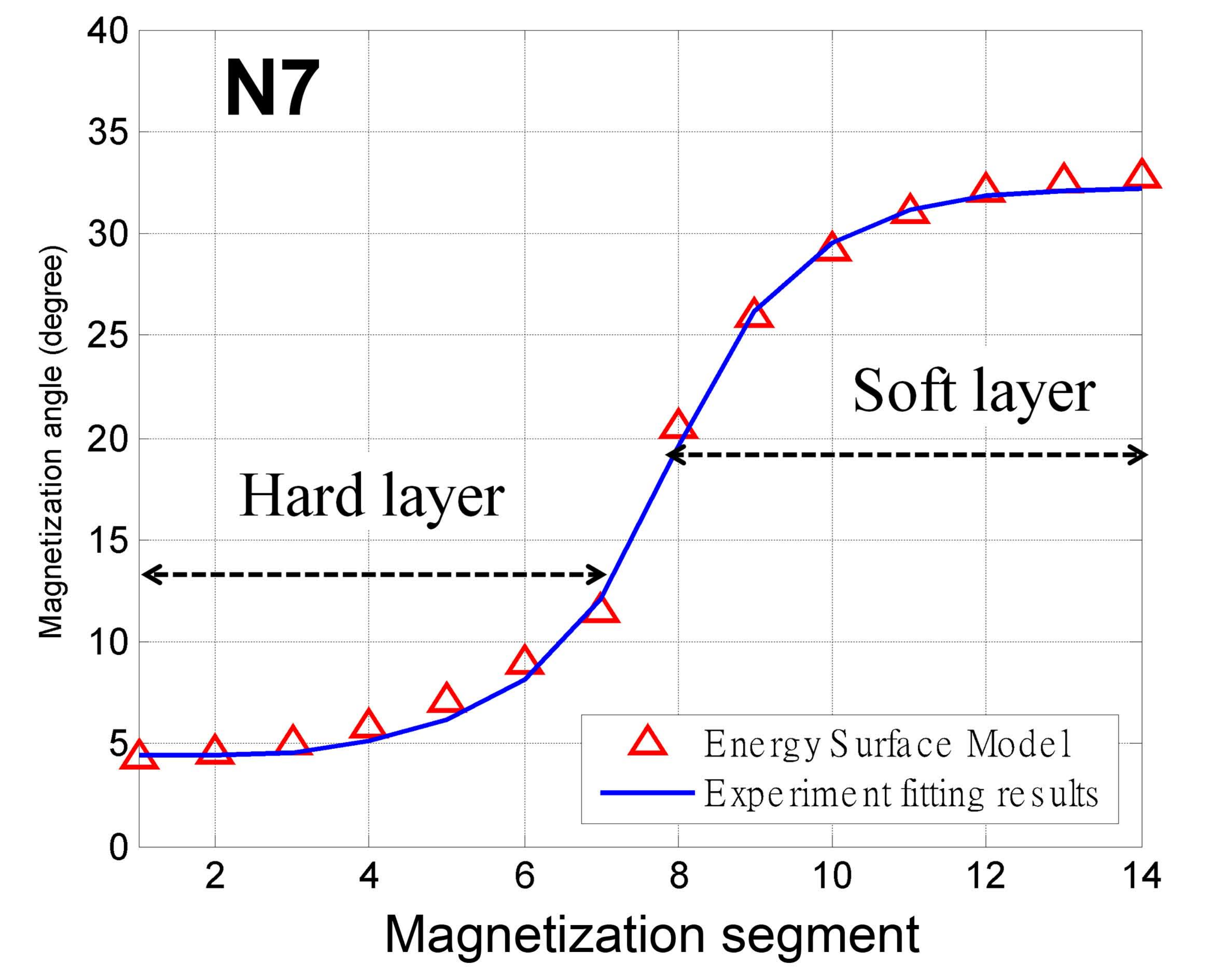

N7
Soft layer
Hard layer
Energy Surface Model
Experiment fitting results
Magnetization angle (degree)
Magnetization segment
0
5
10
15
20
25
30
35
40
2
4
6
8
10
12
14